Cytotechnology **27:** 95–111, 1998.

Intracellular distribution of anthracyclines in drug resistant cells

Giuseppe Arancia, Annarica Calcabrini, Stefania Meschini & Agnese Molinari
Department of Ultrastructures, Istituto Superiore di Sanità, Viale Regina Elena 299, 00161 Rome, Italy

Received 25 May 1998; accepted 25 May 1998

Key words: anthracyclines, doxorubicin, Golgi apparatus, intracellular transport, multidrug resistance, ultrastructure

Abstract

The unresponsiveness of multidrug resistant tumor cells to antineoplastic chemotherapy is often associated with reduced cellular drug accumulation accomplished by overexpressed transport molecules. Moreover, intracellular drug distribution in resistant cells appears to be remarkably different when compared to their wild type counterparts. In the present paper, we report observations on the intracellular accumulation and distribution of doxorubicin, an antitumoral agent widely employed in chemotherapy, in sensitive and resistant cultured tumor cells. The inherent fluorescence of doxorubicin allowed us to follow its fate in living cells by laser scanning confocal microscopy. This study included flow cytometric analysis of drug uptake and efflux and analysis of the presence of the well known drug transporter P-glycoprotein. Morphological, immunocytochemical and functional data evidentiated the Golgi apparatus as the preferential intracytoplasmic site of drug accumulation in resistant cells, capable of sequestering doxorubicin away from the nuclear target. Moreover, P-glycoprotein has been found located in the Golgi apparatus in drug induced resistant cells and in intrinsic resistant cells, such as melanoma cells. Thus, this organelle seems to play a pivotal role in the intracellular distribution of doxorubicin.

Abbreviations: DAU: daunomycin; DOX: doxorubicin; EELS: electron energy loss spectroscopy; ESI: electron spectroscopic imaging; IDX: 4′-deoxy-4′-iododoxorubicin; LRP: lung resistance protein; LSCM: laser scanning confocal microscopy; MDR: multidrug resistance; MRP: multidrug resistance related protein; Pgp: P-glycoprotein; WGA: wheat germ agglutinin.

Introduction

Most of the chemotherapeutic compounds used in cancer treatment exert their cytotoxic action by multifactorial mechanisms which involve several subcellular targets. The identification of these targets can provide new understanding of cytotoxic action mechanisms and can suggest innovative strategies in anticancer chemotherapy. In fact, the neoplastic cell sensitivity to certain anticancer agents could be enhanced by modifying the subcellular targets and then the cell response to the treatment.

In this context, studies on the intracellular localization of antitumoral drugs in cancer cells may provide useful contributions. Moreover, multidrug resistant (MDR) cells are generally characterized by reduced cellular drug accumulation and different intracellular drug distribution compared with their parental sensitive counterpart. Thus, a detailed knowledge of the drug disposition in various cell types exhibiting different degrees of resistance may provide an insight into the mechanisms underlying multidrug resistance and suggest pharmacological strategies for its therapeutic circumvention.

To this aim, several methodologies have been developed and applied in order to study subcellular drug localization with improved resolution. One approach is to separate the various cellular compartments and to measure the relative drug contents. This method, however, might introduce artifacts due to the possible dislocations of the drug molecules during the fractioning procedures.

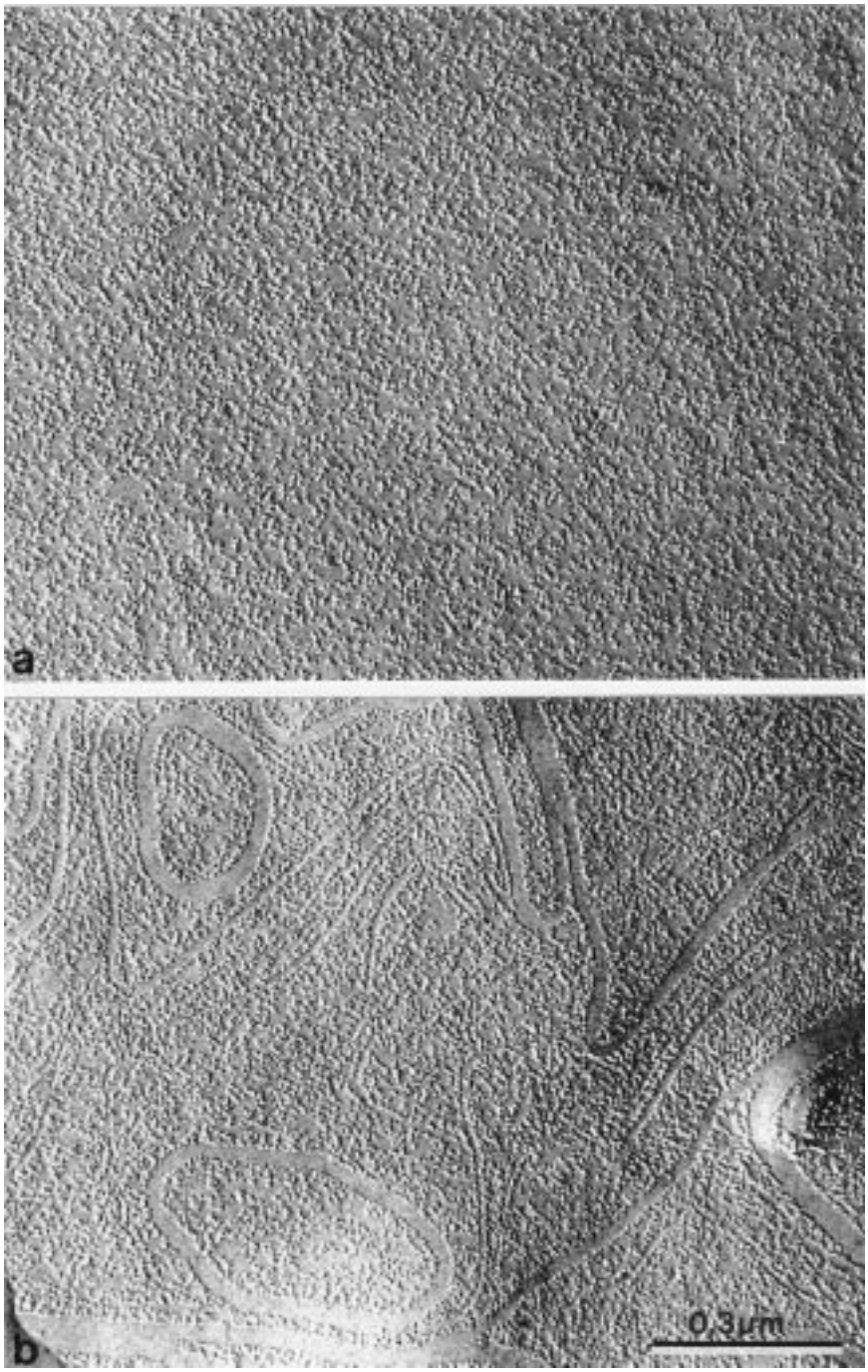

Figure 1. Effect of treatment with 100 μM DOX on the intramembrane particle (IMP) distribution of the plasma membrane of human erythrocytes. (a) Protoplasmic fracture face of the plasma membrane of untreated erythrocyte. The IMPs appear to be randomly distributed. (b) In DOX treated cells, the fracture face is characterized by the presence of numerous particle-free domains with different geometry.

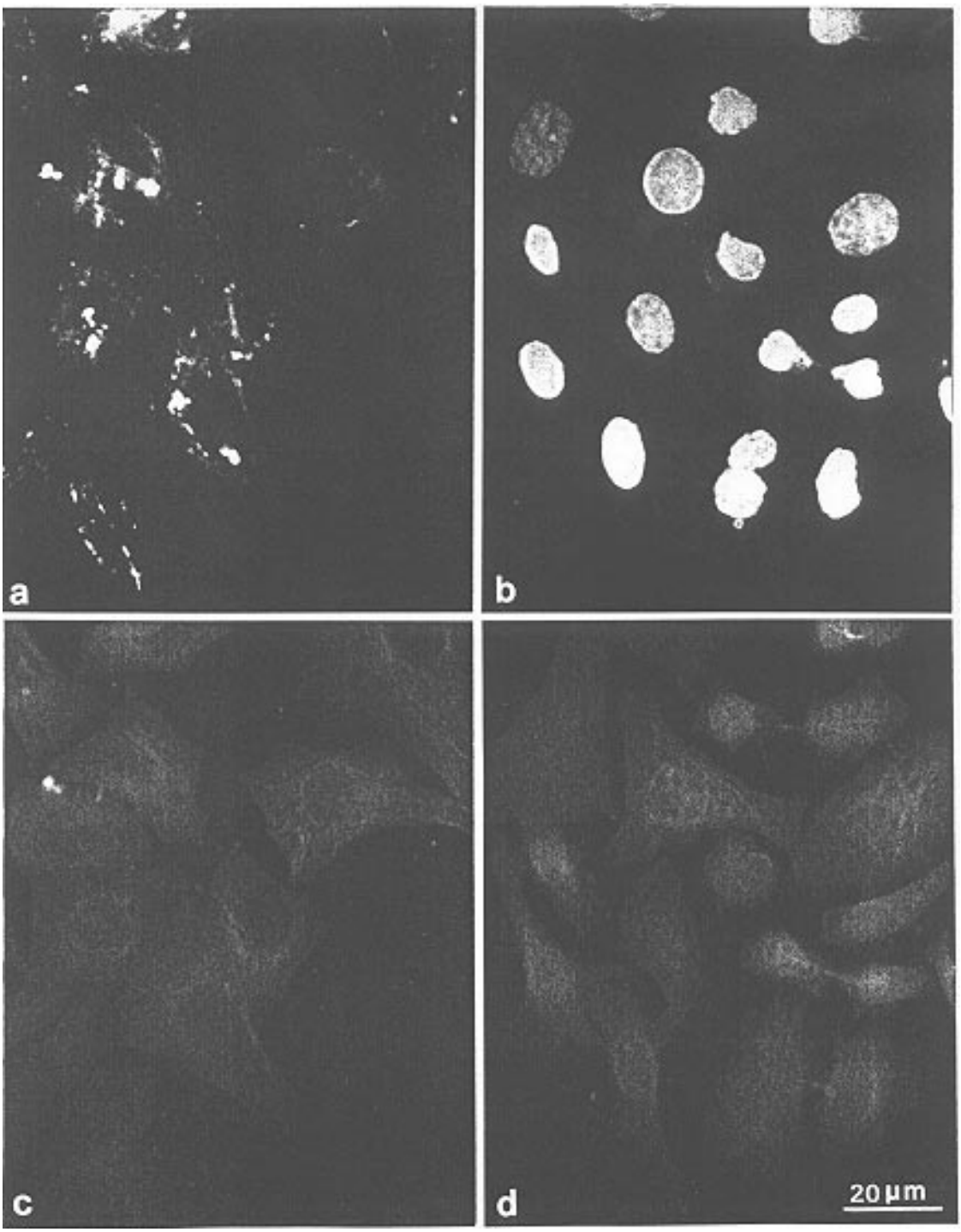

Figure 2. Double immunofluorescence of the cytoskeleton of human breast carcinoma cells (CG5). (a) CG5 control cells: actin microfilaments labelled with FITC-phalloidin appear to be organized in stress fibers and little surface ruffles. (b) After treatment with high dose of anthracycline, the stress fibers disappeared and polymerized actin reorganized in long filamentous protrusions. The anthracycline excited at 488 nm gave the strong fluorescent signal from the nucleus. (c) CG5 control cells (the same field of a): the microtubular network labelled with monoclonal anti-tubulin and rhodamine-linked antimouse antibodies. (d) After treatment with high dose of anthracycline the network collapsed around the nucleus. The signal of anthracycline localized in the nucleus, excited at 515 nm, gave the same red fluorescent signal of rhodamine.

When the antitumoral agent is inherently fluorescent, such as anthracycline antibiotics, fluorescence microscopy, both conventional and confocal, can be usefully employed to study the drug subcellular localization (Coley *et al*., 1993; Meschini *et al*., 1994). Confocal microscopy has several advantanges over conventional fluorescence microscopy, mainly in terms of elimination of out of focus epifluorescence and greater resolution (White *et al*., 1987; Wilson, 1990). Secondary ion mass spectrometry (SIMS) microscopy has also been used to localize and quantify the ^{127}I of the iodinated anthracycline 4′-iododeoxyrubicin in cells from biopsies of patients treated with this drug (Fragu *et al*., 1992). More recently, sophisticated electron microscopic methods have been employed to assess the presence or absence of a drug within clearly identifiable cellular organelles in order to locate precisely where it accumulates. In particular, electron energy-loss spectroscopy (EELS) and electron spectroscopic imaging (ESI) have been applied to assess the location of iodine-containing antitumoral drugs with electron microscopic resolution (Huxham *et al*., 1992; Diociaiuti *et al*., 1997).

In the present paper we report observations, mainly performed by cytometric, morphological and ultrastructural methods, on the intracellular accumulation and distribution of anthracyclines in different cell lines, both sensitive and with different degrees of intrinsic or acquired resistance. The expression of the well known drug resistance marker P-glycoprotein (Pgp) has also been investigated in an attempt to clarify the influence of this transport protein on subcellular drug distribution and, thus, on cell sensitivity to the cytotoxic compounds.

Materials and Methods

Cells

Red blood cells were obtained from healthy donors as described elsewhere (Arancia *et al*., 1988). After treatment with 100 μM doxorubicin (DOX) (Adriblastina, Pharmacia, Milan, Italy), erythrocytes were processed for freeze-fracture electron microscopy, as previously described (Arancia *et al*., 1988).

The parental drug-sensitive human breast cancer MCF-7 cell line (MCF-7 WT) and its derivative MDR variant (MCF-7 DX) were kindly provided by Dr. K. Cowan from NCI, Bethesda, Maryland, USA. These cells were grown as monolayers in RPMI 1640

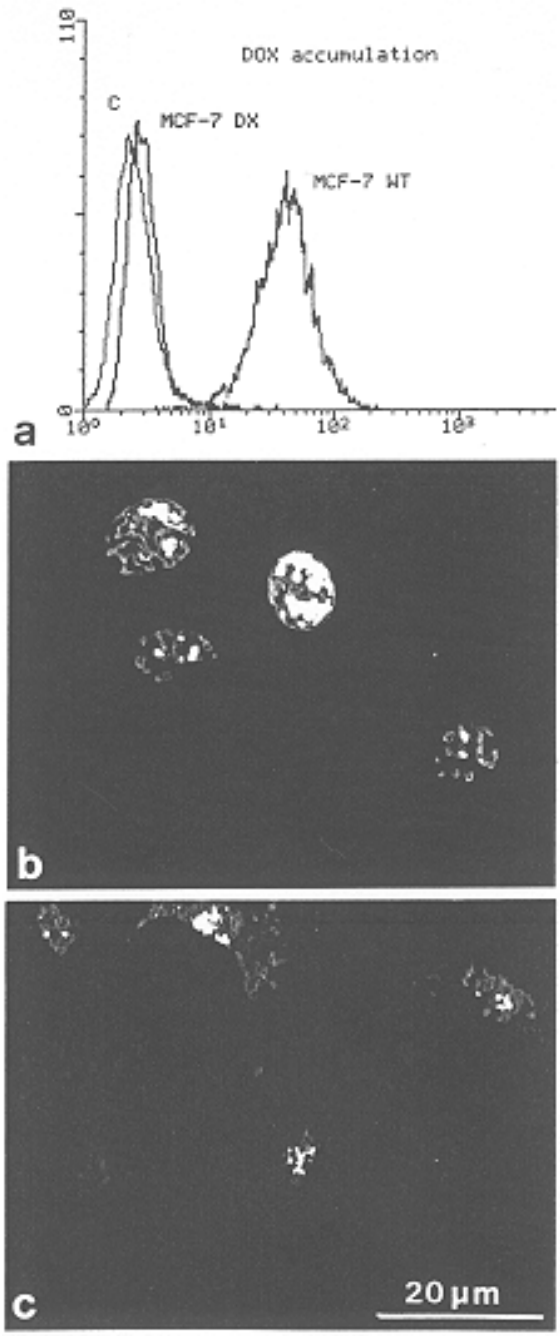

Figure 3. (a) Flow cytometric determination of DOX accumulation for 1 h. Red and green peaks represent drug fluorescence in MCF-7 WT and MCF-7 DX cells, respectively. Black peak represents autofluorescence of untreated cells. In wild type cells the fluorescence intensity (abscissa), due to the intracellular drug content, was much higher than in resistant cells. (b, c) Intracellular drug distribution in MCF-7 WT (b) and MCF-7 DX (c) cells treated with DOX and observed under living conditions by confocal microscopy. In sensitive cells the fluorescent drug molecules were localized preferentially in the nuclei whereas in resistant cells DOX appeared to be exclusively located within the cytoplasm.

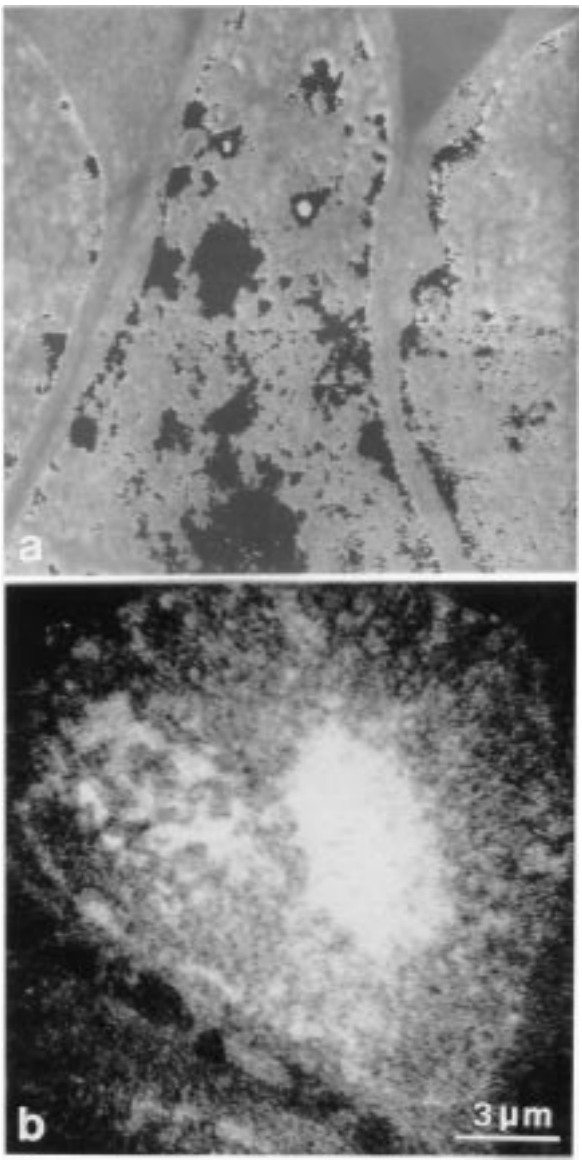

Figure 4. EELS imaging of IDX in MCF-7 WT (a) and MCF-7 DX (b) cells. With this spectroscopic method, iododoxorubicin can be detected due to the presence of the iodine atom in the drug molecule. In (a) the iodine mapping (black signal) revealed the preferential localization of IDX within the nuclei of sensitive MCF-7 cells. The iodine signal was never detected in resistant cells (b).

medium (Flow Laboratories, Irvine, Scotland) supplemented with 10% fetal calf serum, 1% L-glutamine and 0.1% gentamicin at 37 °C in a 5% CO_2 humidified atmosphere in air. MCF-7 DX cells were grown in complete medium containing 10 μM DOX.

Established human melanoma cell lines (M14, H14, JR8) were grown in RPMI 1640 medium supplemented with 1% non essential aminoacids, 1% L-glutamine, 100 IU mL^{-1} penicillin, 100 IU mL^{-1} streptomycin and 10% fetal calf serum at 37 °C in a 5% CO_2 humidified atmosphere in air.

The parental drug-sensitive human colon carcinoma LoVo cell line was grown in Ham's F12 medium (Flow Laboratories) supplemented with 10% fetal calf serum, 1% L-glutamine and vitamins at 37 °C in a 5% CO_2 humidified atmosphere in air.

Human breast carcinoma cells (CG5) were cultured at 37 °C in Dulbecco's modified Eagle's medium (DMEM), supplemented with 1% non essential amino-acids, 1% L-glutamine, 100 IU mL^{-1} penicillin, 100 IU mL^{-1} streptomycin and 10% fetal calf serum.

Cytoskeleton immunolabelling

For the detection of microtubules and actin filaments, cells grown on coverslips were fixed with 3.7% formaldehyde in phosphate buffer solution (PBS), pH 7.4, for 10 min at room temperature. After being washed in the same buffer, the cells were permeabilized with 0.5% Triton X-100 (Sigma Chemicals, St. Louis, MO) in PBS for 10 min at room temperature.

For actin detection, cells were stained with fluorescein-phalloidin (Sigma Chemicals) at 37 °C for 30 min.

For tubulin labelling, cells were incubated with anti-tubulin (α+β) monoclonal antibody (Amersham International plc, Little Chalfont, U.K.) at 37 °C for 30 min. After washing in phosphate buffer, incubation with a rhodamine-linked sheep anti-mouse IgG (Amersham International plc) at 37 °C for 30 min was performed.

Cytotoxicity studies

The clonogenic survival test was used to determine the cell sensitivity to DOX, DOX plus verapamil or DOX plus cyclosporin A. 700 cells were plated in tissue culture dishes (60 mm) and allowed to attach for 48 h before treatment with 1.7 μM (1 μg mL^{-1}) DOX (Pharmacia) for 1 h in the presence or in the absence of 10 μM verapamil (Sigma Chemicals) or 5 μM cyclosporin A (Sigma Chemicals). After 8 days of incubation, cell colonies were fixed with 95 ° ethanol for 15 min and stained with a solution of methylene blue in 80% ethanol for 1 h. Only colonies composed of more than 50 cells were evaluated. The surviving fraction was calculated by dividing the absolute survival of treated cells by the absolute survival of control cells.

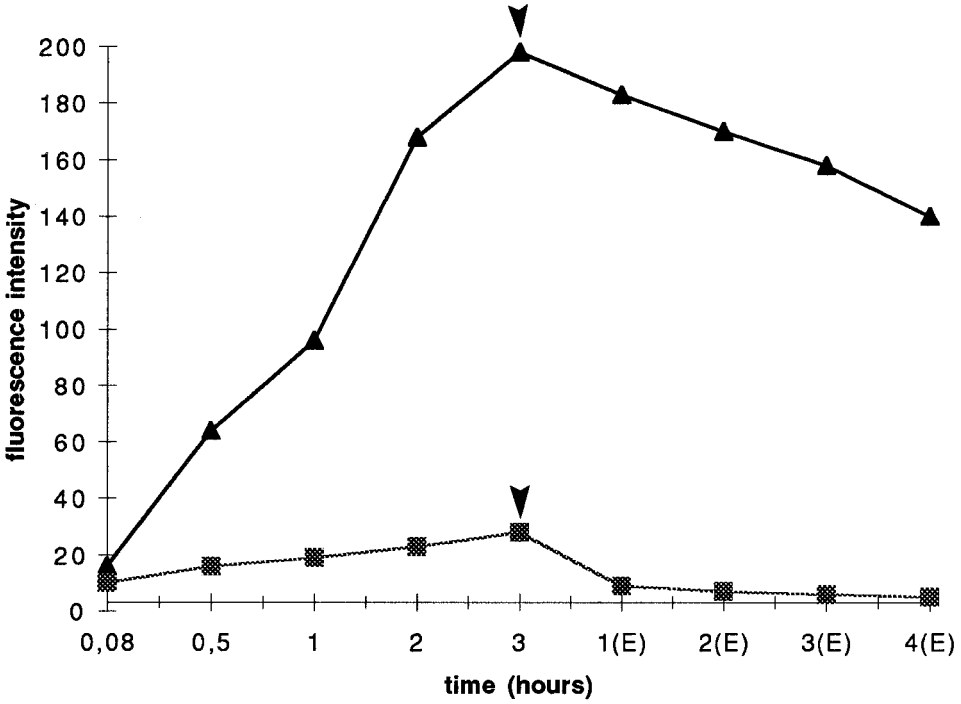

Figure 5. Time course accumulation and efflux of DOX in MCF-7 WT (▲) and MCF-7 DX (■) cells obtained by flow cytometry. Accumulation was performed for 3 h, efflux (E) for 4 h. The arrows indicate the beginning of drug efflux.

Anti-Pgp MAb

MAb MM4.17 (Cianfriglia *et al.*, 1994) which recognizes a human-specific epitope on the extracellular domain of the MDR1-P-glycoprotein isoform, was used in this study. Its optimal concentration for flow-cytometry and immunocytochemistry studies was 50 μg mL^{-1}.

Flow cytometry

All flow cytometric analyses were carried out on cell suspensions (10^6 cells mL^{-1}) obtained by incubating cell cultures with EDTA and trypsin solutions.

For determination of cell surface P-glycoprotein, the cells were incubated for 30 min at 4 °C with MAb MM4.17 (50 μg mL^{-1}). After washing with ice-cold PBS containing 10 mM NaN_3, 1% bovine serum albumine (BSA; Sigma Chemicals) and 0.002% EDTA, cells were incubated for 30 min at 4 °C with F(ab′)$_2$ fragment of goat anti-mouse IgG fluorescein-conjugate (Sigma Chemicals) at a working dilution of 1:50. After washing, cells were immediately analyzed.

To detect intracellular expression of P-glycoprotein, cell suspensions were fixed with 2% paraformaldehyde in PBS for 10 min at 4 °C. Then the samples were permeabilized by adding 0.05% Triton X-100 for 10 min at 4 °C. The incubations with primary antibody (MAb MM4.17) and secondary antibody (F(ab′)$_2$ fragment of goat anti-mouse IgG fluorescein-conjugate) were performed for 30 min at 4 °C. For both surface and intracellular Pgp labelling experiments, negative controls were obtained by incubating the samples with mouse IgG2a isotypic globulins (Sigma Chemicals).

For drug accumulation studies, cell cultures were exposed to 1.7 μM DOX at 37 °C up to 30 h. For Pgp functionality studies, cells were preincubated with 10 μM verapamil or 5 μM cyclosporin A at 37 °C for 15 min. Then, 1.7 μM DOX was added to the cultures at 37 °C up to 30 h. At the various incubation times, cells were harvested, washed in ice-cold PBS and immediately analyzed.

For drug efflux studies, cell cultures were treated with 1.7 μM DOX for 4 h at 37 °C, washed with ice-cold PBS and then reincubated up to 30 h at 37 °C in drug-free medium, with or without modulators as described above. The samples were then processed for analysis of the drug content as in DOX accumulation experiments.

Fluorescence was analyzed with a FACScan flow cytometer (Becton Dickinson, Mountain View, CA)

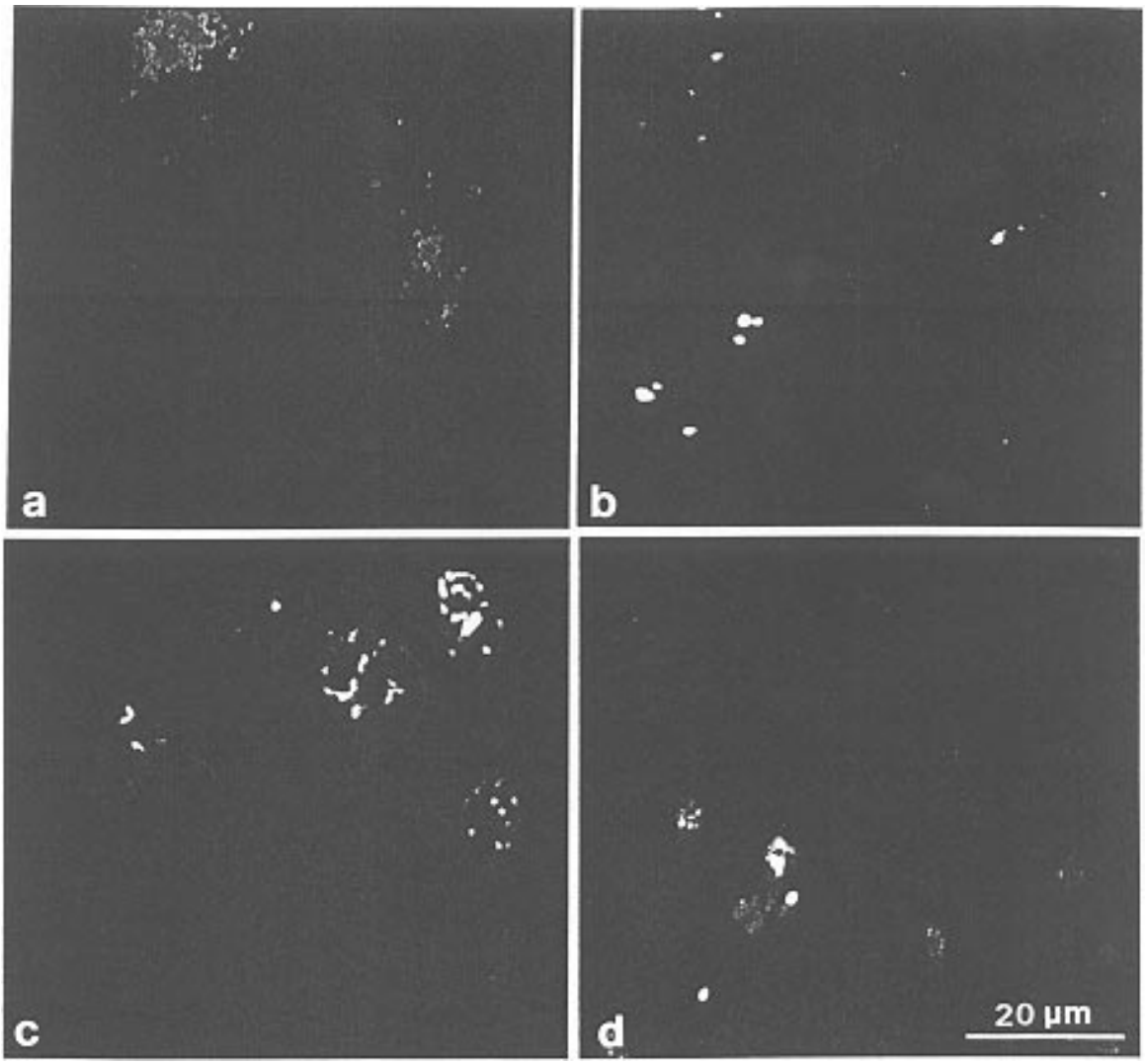

Figure 6. LSCM of intracellular DOX distribution in MCF-7 WT (a, c) and MCF-7 DX (b, d) cells, after 15 (a, b) and 30 min (c, d) of treatment. The different pattern of drug localization between sensitive and resistant cells is well visible (see text for detailed description).

equipped with a 15 mW, 488 nm, air-cooled argon ion laser. The fluorescence emissions of fluorescein and doxorubicin were collected through 530 and 575 nm band-pass filters, respectively, and acquired in log mode. For DOX accumulation and efflux studies, drug fluorescence intensity was expressed as the mean channel and plotted versus time.

Fluorescence microscopy

To detect cell surface P-glycoprotein expression, cells grown on coverslips were incubated with MAb MM4.17 (50 μg mL^{-1}) at 4 °C for 30 min. After washing in phosphate buffer, cells were incubated with goat anti-mouse IgG fluorescein-linked antibody (IgG-FITC; working dilution 1:20; Sigma Chemicals) at 4 °C for 30 min.

To detect intracellular expression of P-glycoprotein, cells were fixed with freshly prepared 3.7% formaldehyde in PBS for 10 min at room temperature. After washing in the same buffer containing 2% BSA, cells were permeabilized with 0.5% Triton X-100 in PBS for 5 min and then incubated with specific MAbs at 37 °C for 30 min. After several washes in PBS, cells were incubated again for 30 min with goat anti-mouse IgG-FITC, at a working dilution of 1:20. Mouse IgG2a isotypic globulins (Sigma Chemicals) were used in negative control samples.

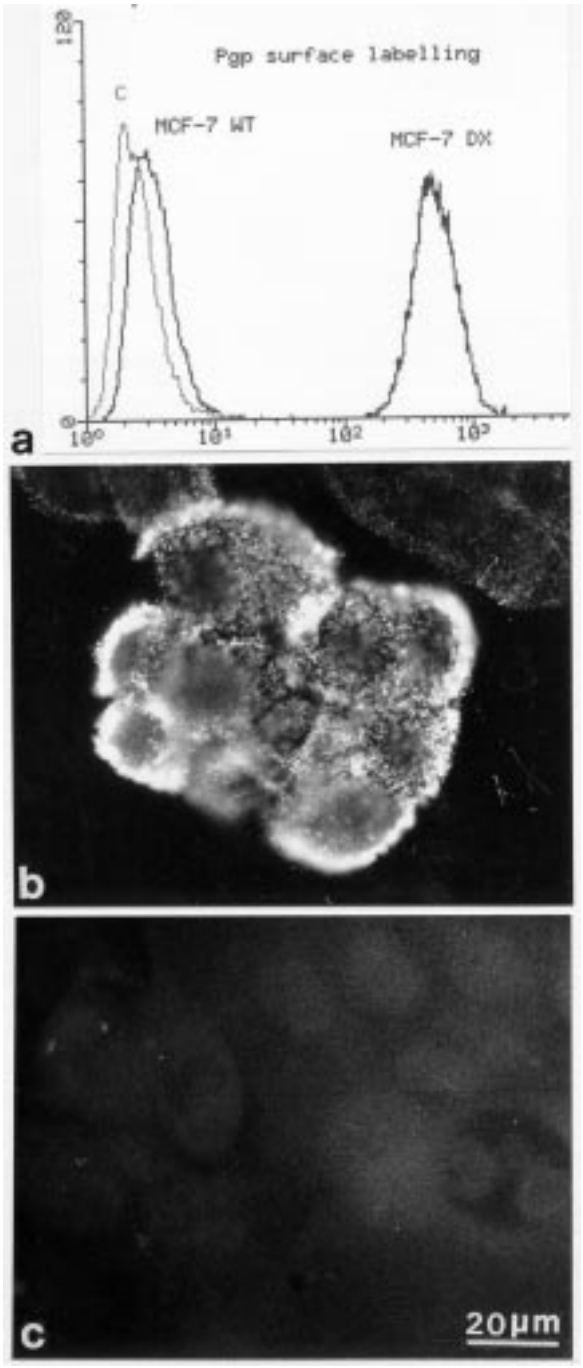

Figure 7. (a) Flow cytometric analysis of surface Pgp expression. The number of cells (ordinate) is plotted versus the fluorescence intensity (abscissa) of the cells. Peak C represents the negative control obtained by incubating cells with an isotypic irrelevant antibody. The fluorescence profile of MM4.17-labelled sensitive cells (MCF-7 WT) and that of negative control (C) were almost coincident. On the contrary, resistant cells (MCF-7 DX) were positive for MAb MM4.17 and the fluorescence signal was 2-logs different from control sample. Immunofluorescence microscopy observations confirmed an high surface Pgp expression on MCF-7 DX cells (b), while MCF-7 WT cells did not show any reactivity against MM4.17 antibody (c).

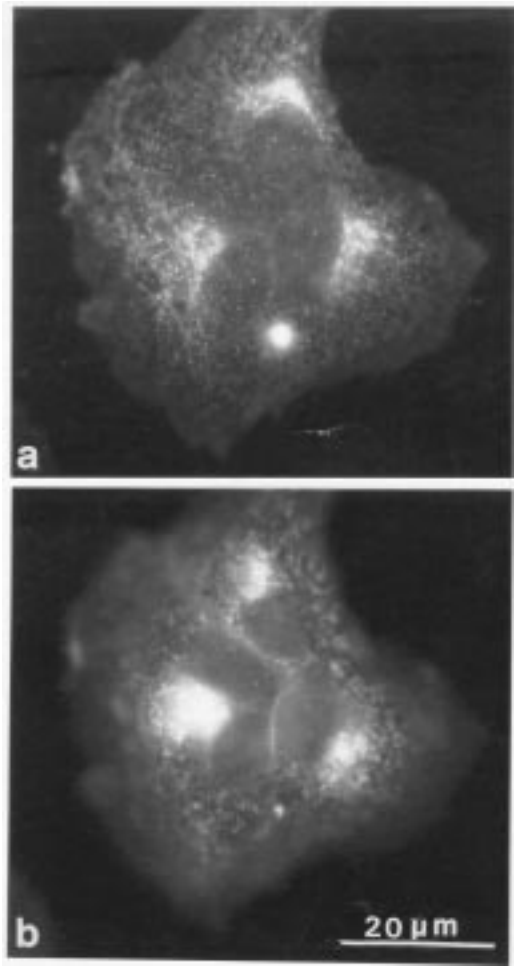

Figure 8. Double labelling of Golgi apparatus (a) and P-glycoprotein (b) in MCF-7 DX cells. The Golgi-Pgp colocalization in the same perinuclear region appeared to be quite well evident.

For Golgi apparatus staining, the method by Coan *et al.* (1993) was used. Briefly, after three washes in PBS, the cells were fixed and permeabilized with methanol at –20 °C for 10 min and then incubated with 50 mg mL^{-1} in PBS of wheat germ agglutinin-fluorescein linked (WGA-FITC; Sigma Chemicals) for 30 min at room temperature.

For the double-labelling of Golgi apparatus and P-glycoprotein, the cells were first labelled for the Golgi apparatus, following the method described above. After washing with PBS, the cells were incubated with MAb MM4.17 for 30 min at room temperature and, following several washes in PBS, incubated with a rhodamine-linked goat anti-mouse IgG (Sigma Chemicals) (working dilution 1:30). After washing, cover-

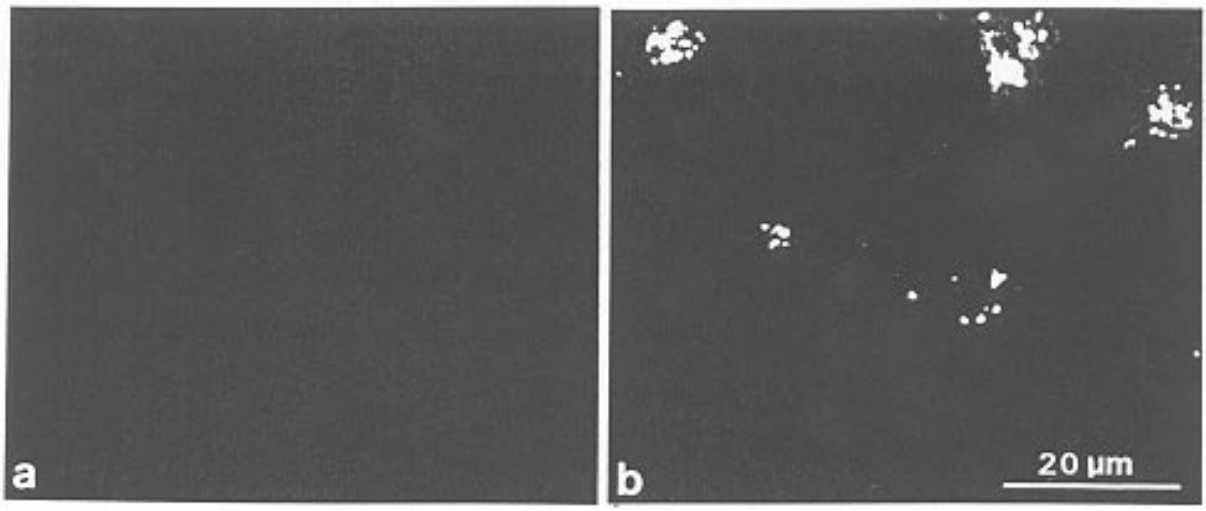

Figure 9. LSCM of intracellular DOX distribution in MCF-7 DX cells in the absence (a) and in the presence (b) of verapamil. This MDR reverting agent was able to inhibit the efflux of the drug. In fact, when DOX treatment was performed in association with verapamil (b), a stronger cytoplasmic signal was detected when compared to administration of DOX alone (a).

slips were mounted with glycerol-PBS (1:2) containing 2.5 mg mL^{-1} propyl gallate.

The observations were performed with a Nikon Microphot-SA fluorescence microscope (Nikon, Tokjo, Japan).

Confocal microscopy

The analysis of the intracellular distribution of DOX was carried out on living cells, grown on coverslips and mounted on glass microscope slides, in the presence of the culture medium. Cells were incubated with 1.7 μM DOX at 37 °C for incubation times ranging from 5 min to 30 h.

In order to avoid cell damage, the image acquisitions, recorded as section series, were made quickly on several cells present on different coverslips for each sample, acquiring signals from one field per coverslip. The observations were carried out using a Molecular Dynamics Sarastro 2000 laser scanning confocal microscope (Molecular Dynamics, Sunnyvale, CA). The excitation and emission wavelengths employed were 488 and 510 nm, respectively. The acquisition parameters were: objective 60x/1.40, image size of 1024×1024 pixels, pixel size of 0.17 μm, step size of 1.1 μm. To show both surface and internal cell structures, the section series were processed by look-through projection method. Voxel intensities along projection rays were summed: the rays lay perpendicular to the plane of the monitor screen. This method is also termed 'extended focus' because the resulting images appear to have gathered from a transparent specimen by a lens with large depth of focus. The acquisitions were recorded employing the pseudo-color intensity representation.

EELS imaging

Electron Energy Loss Spectroscopy (EELS), performed in a classical TEM environment, is a non-destructive spectroscopic technique for the characterization of the chemical properties of different samples. EELS uses the information carried by the transmitted electrons at the exit surface of the specimen. The scattering events suffered by the outgoing electrons are recorded. By evaluating the energy loss of electrons an EELS spectrum can be obtained which gives information about the chemical composition or electronic binding energies. Moreover, images can be obtained by collecting only electrons that suffered energy loss characteristic of an atomic species. This technique, namely Electron Spectroscopic Imaging, is able to obtain elemental maps with a resolution comparable to TEM resolution.

EELS imaging was performed on both sensitive and resistant MCF-7 cells, treated with 4′-deoxy-4′-iododoxorubicin (IDX), fixed with 2.5% glutaraldehyde and embedded by classical procedure. Unstained ultrathin sections were analyzed by a dedicated Zeiss EM902 transmission electron microscope (Diociaiuti *et al*., 1997). The three-windows procedure was used in the iodine analysis. Energy windows of 540–580,

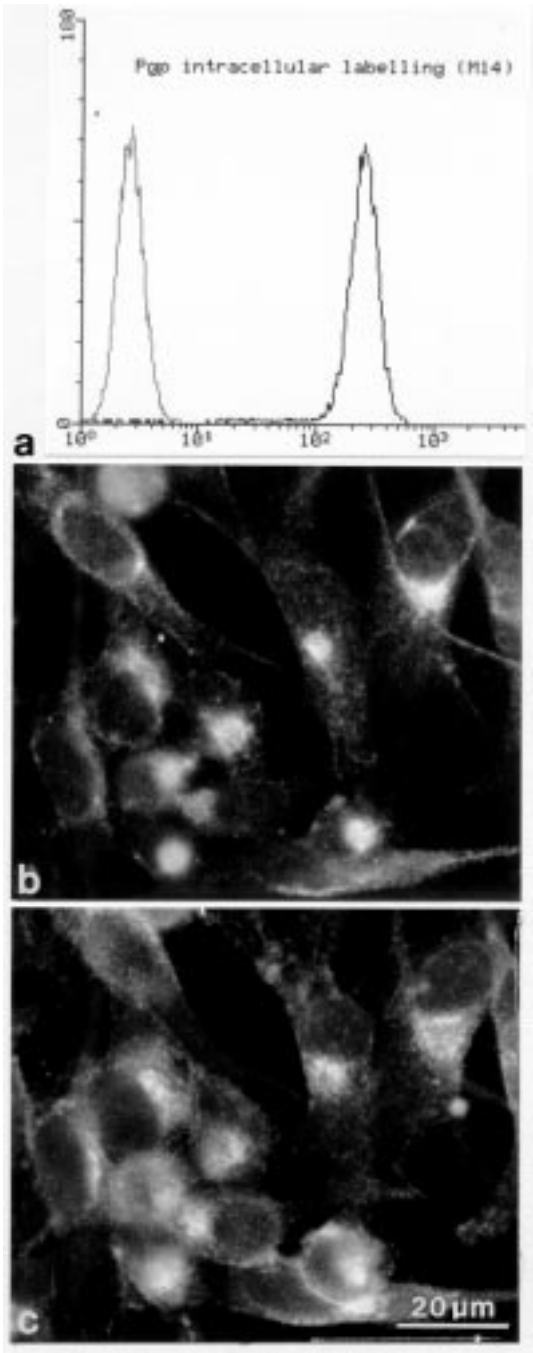

Figure 10. (a) Flow cytometric analysis of Pgp intracellular expression shows a strong reactivity in permeabilized M14 cells. The number of cells (ordinate) is plotted versus the fluorescence intensity (abscissa) of the cells. The grey peak represents the negative control obtained by incubating cells with an isotypic irrelevant antibody. Double staining experiments, performed using Mab MM4.17 followed by rhodamine-linked goat anti-mouse IgG for Pgp intracellular labelling (b) and with fluorescein-linked WGA for Golgi staining (c) confirmed that Pgp could be located in the Golgi apparatus of human melanoma cells.

560–600 and 640–680 eV, respectively, were used. Reference images with high contrast were acquired by energy filtering at about 250 eV. Iodine map was colored in black and superimposed on the reference image.

Results and Discussion

Subcellular targets of anthracyclines

Most of the studies on the intracellular accumulation and distribution of antitumoral drugs in cancer cells have been performed using anthracyclines, a well known class of cytotoxic compounds widely employed in anticancer chemotherapy. Such studies are facilitated by the high inherent fluorescence of the anthracycline molecules, in that their presence in cellular material can be easily detected and visualized by fluorimetric methods, such as flow cytometry and fluorescence microscopy.

The antitumoral activity of anthracyclines has been attributed mainly to their intercalation between the base pairs of the DNA molecule which can alter the conformation of the nucleic acid, cause DNA fragmentation and induce inhibition of RNA and DNA synthesis (Mizuno *et al.*, 1975; Monparler *et al.*, 1976; Fritzsche *et al.*, 1982; Ralph *et al.*, 1983). However, several studies showed that anthracycline-induced cytotoxicity could be ascribed not only to an effect of the drug on nucleic acids but also on other important cellular structures, such as membranes and cytoskeleton.

As far as cellular membranes are concerned, it has been demonstrated that doxorubicin (DOX, also called adriamycin), the main congener of the anthracycline family, exhibits a specific affinity to negatively charged phospholipids (Duarte-Karim *et al.*, 1976; Goormaghtigh and Ruysschaert, 1984; Henry *et al.*, 1985). Therefore, the lipid composition of the membrane seems to be important for the sensitivity of tumor cells to DOX and for this reason efforts have been directed towards modifying the plasma membrane in order to modulate the interaction with the drug and, subsequently, its cytotoxic action (Guffy *et al.*, 1984). Modifications of the cell surface induced by DOX, such as changes in the membrane fluidity, lipid composition, expression of membrane-bound enzymes as well as other cell surface functional properties, have been widely demonstrated (Tritton and Yee, 1982; Siegfried *et al.*, 1983; Oth *et al.*, 1987).

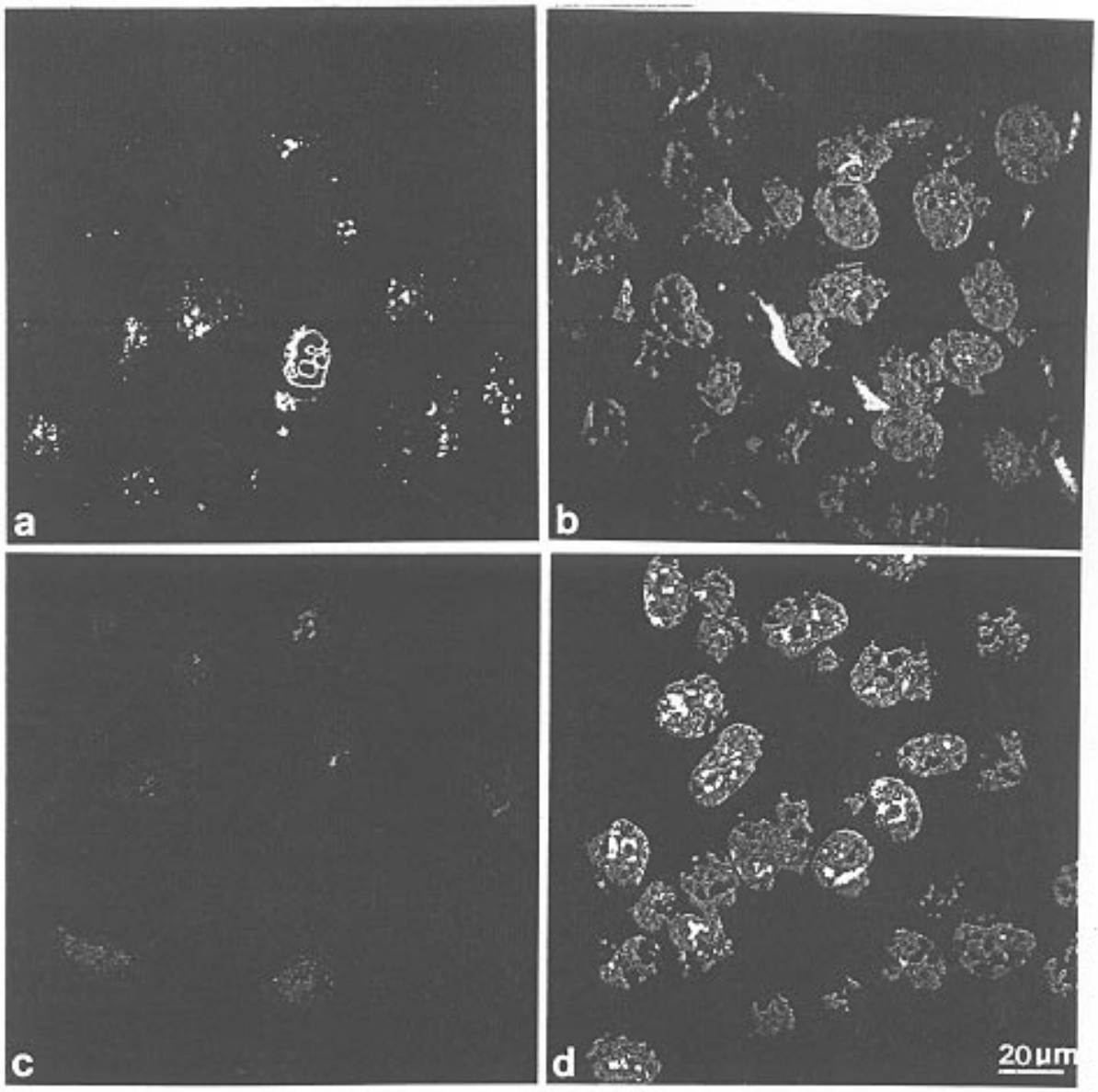

Figure 11. LSCM of the intracellular DOX distribution in M14 cells. (a, b) Cells treated with DOX for 15 min (a) and for 1 h (b). (c) DOX distribution after 24 h efflux. (d) DOX distribution after 24 h efflux in the presence of cyclosporin A (see text for detailed description).

In our previous investigations performed by ultrastructural and spectroscopic methods on the anthracycline-membrane interaction, we found that the incorporation of DOX molecules within both lipid layers induces remarkable changes in some ultrastructural and physical parameters of the plasma membrane with consequent alterations in the functional properties (Arancia *et al*., 1988; Diociaiuti *et al*., 1991a; Diociaiuti *et al*., 1991b; Arancia *et al*., 1994; Arancia *et al*., 1995).

In particular, freeze-fracture electron microscopy revealed a very unusual distribution of protein intramembrane particles in membranes of human erythrocytes treated with DOX when compared to the control ones (Figure 1a). Numerous smooth areas of variable geometry were detectable on a large part of the protoplasmic fracture face of treated erythrocytes (Figure 1b). A number of evidences supported the hypothesis that the smooth areas might represent a vi-

sualization of the DOX molecules incorporated inside the lipid bilayer (Arancia *et al.*, 1995).

Concerning the cytoskeleton, several studies showed that the anthracycline-induced cardiotoxicity could be ascribed to an effect of the drug on the cytoskeletal apparatus of cardiac cells (Lewis and Gonzales, 1986; Rabkin and Sunga, 1987). We found that both doxorubicin and daunomycin (DAU) induced multinucleation and spreading phenomena in cultured cells, interferring with the organization of microtubules and microfilaments (Molinari *et al.*, 1990). In particular, it was observed that DAU was able to modulate the microtubule reassembly in human melanoma cells treated with colcemid and that treatment with DAU induced the stabilization of the microtubules, making them more resistant to the action of antimicrotubular agents (Molinari *et al.*, 1991). Figure 2 shows the actin and tubulin arrangements (a and c, respectively) in control CG5 cells and the relative modifications induced by the exposure to 50 μM DOX for 2 h (b and d, respectively).

These observations seem to confirm the cytoskeletal apparatus as another important target involved in the mechanism of action of anthracyclines.

Intracellular accumulation and distribution of DOX in wild type sensitive breast carcinoma cells and in their derivative MDR variants

Cells expressing the MDR phenotype can be selected *in vitro* by prolonged exposure to various antitumoral drugs. The acquisition of MDR is often associated with changes in both intracellular drug content and disposition (Fojo *et al.*, 1985; Willingham *et al.*, 1986; Schurrhuis *et al.*, 1991; Coley *et al.*, 1993). These changes appear to be mediated by different protein transporters which are generally overexpressed in MDR cells.

We have compared the subcellular localization of anthracycline molecules in wild type human breast cancer cells (MCF-7 WT) and in their derivative MDR variants (MCF-7 DX). Moreover, the relationship between expression of the well-known drug resistance marker P-glycoprotein (Pgp) and drug distribution in this cell model has been investigated.

As expected, flow cytometric analysis of DOX accumulation revealed that in MCF-7 WT cells the fluorescence intensity due to the intracellular drug content was much higher than in MCF-7 DX cells (Figure 3a). Besides this difference in intracellular drug accumulation, wild type and resistant cells were found to be remarkably different in the distribution of

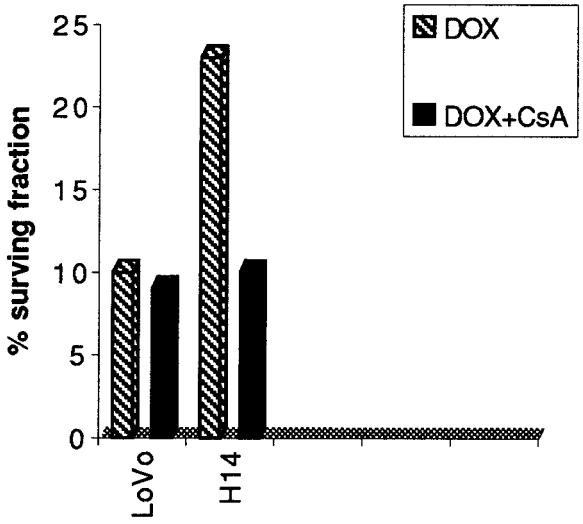

Figure 12. Sensitivity to DOX of H14 and LoVo cells in the absence and in the presence of cyclosporin A (CsA). H14 cells treated with DOX alone showed a survival fraction significantly higher than that of LoVo cells. CsA induced a reduction in cell survival in melanoma cells and no effect in LoVo cells.

the anthracycline compound. When sensitive MCF-7 WT cells were treated with 1.7 μM DOX for 1 h and observed under living conditions by laser scanning confocal microscopy (LSCM), the fluorescent drug molecules localized preferentially in the nuclei (Figure 3b). In MCF-7 DX cells DOX appeared to be exclusively located within the cytoplasm, while the nuclei were completely negative (Figure 3c).

Changes in intracellular drug localization, and in particular decrease in the nuclear/cytoplasmic ratio of doxorubicin fluorescence, were detected in several resistant cell lines (Broxterman *et al.*, 1990; De Lange *et al.*, 1992). The shift in the ratio nuclear drug/cytoplasmic drug has been reported to be related to resistance to doxorubicin (2.8–3.6 in sensitive cells vs. 0.1–0.4 in cells with 70-fold higher level of resistance) (Schurrhuis *et al.*, 1993). Biophysical studies (Frezard and Garnier-Suillerot, 1991) demonstrated that the intercalation between the base pairs of DNA induced the partial quenching of DOX fluorescence. However, drug molecules bound to the negatively charged phosphate of DNA, but not intercalated, gave out a fluorescent signal. According to these studies, high levels of free or phosphate bound DOX are present in the nuclei of parental sensitive cells which appear to be intensely fluorescent. The concentration of the drug in three nuclear states (free, intercalated and phosphate-bound) will reflect a passive equilibrium within the nucleus. Consequently, if

significant levels of DOX were intercalated into the DNA of resistant cells, the proportionally high levels of free and phosphate-bound drug should also be detected and an appropriate fluorescent signal should be observed. Thus, the absence of signal from the nuclei of the drug-resistant cells very strongly suggests that they contain negligible levels of DOX.

The preferential location of the anthracycline molecules within the nuclei of sensitive cells and their absence, or at least very low concentration, in the nuclei of MDR cells were also confirmed by electron energy loss spectroscopy (EELS) imaging (Diociaiuti *et al*., 1997). This method was applied on ultrathin sections of both wild type and resistant MCF-7 cells treated with 4′-deoxy-4′-iododoxorubicin (IDX), an halogenated derivative of DOX, taking advantage of the presence of the iodine atom in this molecule. Figure 4a shows the iodine mapping (black signal), superimposed on the respective reference image, in a representative sensitive MCF-7 cell. The preferential localization of IDX inside the nucleus was well evident. Moreover, the colocalization of the I signals and the chromatine clumps confirmed the intercalation of IDX between the base pair of the nucleic acids (Chaires *et al*., 1982). The I signal was never detected in resistant cells treated with the same IDX dose, as shown in Figure 4b.

The time courses of drug uptake and the subsequent drug efflux performed by flow cytometry on both MCF-7 WT and MCF-7 DX cells revealed remarkable difference in the accumulation capability of DOX in the two cell types (Figure 5). When sensitive cells were exposed to 1.7 μM DOX, the fluorescence intensity increased rapidly. Conversely, a very low increase in fluorescence could be detected in resistant cells, revealing a noticeable reduction in drug uptake and/or the existence of potent mechanisms of drug efflux. After 3 h of DOX exposure the intensity of fluorescence emitted by the molecules of the antitumoral drug present inside sensitive cells was about eight time higher than the intensity from the resistant counterparts. When DOX-treated cells were allowed to recover in drug free medium, the fluorescent signal in MCF-7 DX cells after 1h recovery was approximately the same as the negative control, indicating a complete drug efflux, whereas in wild type MCF-7 cells a low reduction (about 30%) was revealed after recovery for 4 h.

Besides differences in intracellular drug concentration, sensitive and resistant cells showed a different pattern of drug localization during the early phases of DOX uptake, as revealed by LSCM. In MCF-7 WT cells, observed after 15 min of drug exposure, DOX was localized preferentially in cytoplasmic vesicles in the perinuclear area and a weak positivity was visible inside the nuclei (Figure 6a). After the same period of treatment, the nucleus of the MCF-7 DX cells was completely negative with faint fluorescence visible in the cytoplasm (Figure 6b). At 30 min of treatment, the nuclei of sensitive cells displayed a strong positivity and a clear visible fluorescent signal could also be detected in the perinuclear area (Figure 6c). In resistant cells, a weak cytoplasmic signal was observed after 30 min of DOX exposure whereas the nuclei were still negative (Figure 6d).

The different subcellular localization of DOX observed in parental and resistant MCF-7 cells is in good agreement with previous reports which described a very similar anthracycline distribution in a number of cell pairs. A vesicular perinuclear localization of the drug, described as ‘punctate pattern’ in LSCM studies, has been reported in several drug resistant cells (Sehested *et al*., 1987; Beck *et al*., 1989; Keizer *et al*., 1989; Gervasoni *et al*., 1991). Therefore, the transport of the drug by acidic vesicles seems to represent an important aspect of the multidrug resistance phenomenon (Sehested *et al*., 1987). The sequestration of the drug molecules into the intracytoplasmic vesicles can be mediated by transport associated proteins, such as Pgp (Willingham *et al*., 1987; Molinari *et al*., 1994) and MRP (multidrug resistance protein) (Breuninghe r *et al*., 1995), located on the membrane of the cytoplasmic organelles. These transport proteins determine abnormal subcellular compartmentation of anthracyclines, preventing their interaction with the intracellular targets (Gervasoni *et al*., 1991; Boiocchi and Toffoli 1992; Schurrhuis *et al*., 1993). In particular, the removal of the drug from the nucleus in resistant cells may prevent the interaction of the putative cell targets, such as DNA, with the cytotoxic drug (Gervasoni *et al*., 1991; Seidel *et al*., 1995). Notwithstanding, the intracellular compartmentation of anthracyclines could also depend on their lipophilic characteristics or their specific structural properties (Lothstein *et al*., 1992; Duffy *et al*., 1996; Toffoli *et al*., 1996).

Immunocytochemical localization of Pgp in breast carcinoma cells

In order to verify the possible involvement of Pgp in the regulation of drug distribution, the surface and intracellular expression of the drug transporter has been studied using the monoclonal antibody MM4.17

(Molinari *et al*., 1994). MAb MM4.17 recognizes a defined, human-specific epitope on the P-glycoprotein extracellular domain (Cianfriglia *et al*., 1994).

Flow cytometric determination of cell surface Pgp (Figure 7a) showed that MDR variants of MCF-7 cells were positive for MAb MM4.17, which reacted with virtually all the resistant cells, and the fluorescence signal was 2-logs different from control sample. As expected, MCF-7 WT cells did not show any reactivity: in fact, the fluorescence profile of MM4.17-labelled sensitive cells and that of negative control cells were indistinguishable.

Immunofluorescence microscopy observations confirmed the data obtained by flow cytometric analysis. MAb MM4.17 recognized epitopes on the surface of MCF-7 DX cells (Figure 7b) whereas the sensitive parental cells appeared to be completely negative when labelled with the same antibody (Figure 7c).

Then, we examined Pgp intracellular localization on fixed and permeabilized cells: a strong fluorescent signal was observed both in the perinuclear region and on the plasma membrane of MCF-7 DX cells. This suggested that in MDR cells Pgp could be also located in a cytoplasmic region likely to be occupied by the Golgi apparatus (Molinari *et al*., 1994). In order to confirm such a location of Pgp, MCF-7 DX cells were double stained with fluorescein-linked wheat germ agglutinin (WGA) and with MAb MM4.17 followed by rhodamine-linked goat anti-mouse IgG. The double immunofluorescence labelling showed that fluorescein (Figure 8a, Golgi apparatus) and rhodamine (Figure 8b, Pgp) signals were superimposed upon one another in the same perinuclear region. The Golgi-Pgp colocalization was also observed in other MDR cell lines, thus indicating that the location of the drug transporter in the Golgi apparatus was not a feature specific to a single cell type.

Taken all together, these observations were suggestive of an important role played by the Golgi compartment in the intracellular transport of anthracycline molecules and indicated that intracytoplasmic Pgp might have a functional role.

To verify these hypotheses, the intracellular localization of DOX in MCF-7 DX cells treated with DOX alone or in the presence of verapamil, a reversing agent that binds to the transporter with high affinity (Cornwell *et al*., 1987; Safa *et al*., 1987) was studied using LSCM. Resistant cells treated with DOX were able to promptly extrude the drug, showing a very low fluorescent signal after 1h efflux (Figure 9a). Conversely, when DOX treatment was performed in association with verapamil, a strong signal was detected in the cytoplasm, mainly in the perinuclear region corresponding to the Golgi apparatus (Figure 9b).

Our observations, in particular the significant expression of Pgp in the Golgi apparatus where DOX preferentially accumulates (Molinari *et al*., 1994), and those reported by others (Rutherford and Willingham, 1993), seem to demonstrate that Pgp is present on the membrane of the Golgi elements and that it can also actively function in this region as drug transporter.

In addition, it has been reported that Pgp is highly represented not only on the plasma membrane and in the cytoplasm but also in the nuclear envelope and inside the nucleus of MDR cells (Baldini *et al*., 1995). Therefore, the nucleus seems to be another important site for Pgp activity in the regulation of the intracellular DOX distribution in resistant cells. In particular, nuclear Pgp is involved in the active removal of cytotoxic drugs from their intranuclear targets.

In conclusion, the different subcellular accumulation and distribution of DOX in sensitive and resistant cells seem to be the result of combined transport activities exerted by Pgp located in various subcellular compartments of MDR cells.

Intracellular distribution of Pgp and DOX in melanoma cells

Malignant melanoma in its metastatic stage is highly unresponsive to chemotherapy (Koh, 1991). The involvement of transport-associated proteins such as MRP (multidrug resistance related protein) (Zaman *et al*., 1993), LRP (lung resistance protein) (Scheper *et al*., 1993) and the well known multidrug resistance marker Pgp has been investigated (Schadendorf *et al*., 1995). However, the mechanisms underlying intrinsic-MDR of malignant melanoma are yet to be elucidated.

In our recent study (Molinari *et al*., 1998) the presence of Pgp was demonstrated in the cytoplasm of human melanoma cell lines which do not express this transport molecule on the cell surface.

The intracellular expression and localization of Pgp were analyzed on fixed and permeabilized cells by flow cytometry and fluorescence microscopy using MAb MM4.17. Flow cytometric analysis showed that this monoclonal antibody reacted with intracellular epitopes in all three human melanoma cell lines examined (M14, H14, JR8) (Figure 10a). The fluorescence microscopy observations suggested that Pgp could be located in the Golgi apparatus of human melanoma cells. Double-staining experiments, performed with MAb MM4.17 followed by rhodamine-

linked goat anti-mouse IgG and fluorescein-linked WGA confirmed this hypothesis. The double immunofluorescence labelling showed that rhodamine (Figure 10b, Pgp) and fluorescein (Figure 10c, Golgi apparatus) signals were strikingly coincident in the same perinuclear region.

To investigate if Pgp detected in the Golgi apparatus plays a role in drug transport, the intracellular localization of DOX was investigated by LSCM. M14 cells were exposed to 1.7 μM DOX and observed under living conditions at different time intervals (Figure 11). During the first minutes of treatment, the early phase of the drug uptake could be depicted. At 15 min the drug was mainly located in the Golgi apparatus, whereas a weak fluorescence was visible in the nucleus (Figure 11a). In M14 cells treated with DOX for 1 h (Figure 11b) all the nuclei were strongly fluorescent: in most of the cells the drug was concentrated in well defined plasma membrane zones and a residual fluorescence positivity was still visible in perinuclear regions. When DOX treated cells were allowed to recover in drug-free medium, a slow drug efflux occurred. After about 24 h the nuclei appeared to be scarcely positive (Figure 11c). Under this last experimental condition, the intracellular drug distribution was comparable to that observed at the beginning of DOX administration; in fact, in both cases, the drug appeared to be located almost exclusively in the cytoplasm, close to the nucleus.This finding suggests that when DOX concentration is low, the drug molecules are preferentially accumulated in the acidic vesicular structures of the Golgi apparatus, where Pgp epitopes were principally found.

We previously interpreted (Calcabrini *et al*., 1997) the preferential location of DOX in the perinuclear region of M14 cells, observed during both the initial period of the drug uptake and the efflux phase, to be due to the DOX molecules being weak bases. Following the diffusion across the porous nuclear envelope DOX molecules, due to their positive electric charge, localized in acidic vesicles of the *trans* Golgi elements (Rutherford and Willingham, 1993) that bind and are transported along microtubules towards the cell surface (Peterson and Trouet, 1978; Hindenburg *et al*., 1989).

In the light of the results herein reported, the involvement of Pgp localized in the Golgi apparatus in the sequestration of the drug molecules inside the lumen of vesicles has to be considered.

Thus, the effect of two well known MDR modifiers, verapamil and cyclosporin A (Safa *et al*., 1987; Saeki *et al*., 1993) on the intracellular distribution of DOX in melanoma cells has been studied. As observed by LSCM, in cells recovered for 24 h in drug-free medium (Figure 11c) DOX was located preferentially in the Golgi region whereas in the presence of cyclosporin A, DOX was mainly retained into the nucleus (Figure 11d). Such a difference confirms the roles of sequestration, transport and extrusion played by Pgp located on the membranes of Golgi vesicles. In fact, during the efflux in the absence of the MDR modifier, the scarce intranuclear localization of DOX can be attributed to drug concentration gradients between cell compartments, which prevent nuclear accumulation through a reduction in cytoplasmic concentration (Schurrhuis *et al*., 1989). When the efflux occurs in the presence of cyclosporin A, the Pgp function is inhibited resulting in a significant intranuclear drug retaining.

Moreover, both verapamil and cyclosporin A were able to sensitize melanoma cells to DOX. Figure 12 shows the percent cell survival of H14 melanoma cells after treatment with 1.7 μM DOX or DOX plus cyclosporin A. These values are compared with those obtained on wild type colon carcinoma cells (LoVo) under the same treatment conditions. After treatment with DOX alone, H14 cells showed a survival fraction significantly higher than that of LoVo cells, confirming the intrinsic resistance of the melanoma cells to the cytotoxic effect of the anthracycline compound. When DOX treatment was performed in association with cyclosporin A, a reduction in cell survival was detected in melanoma cells whereas, as expected, no effect of the MDR modulator could be observed in LoVo cells.

In conclusion, Pgp located in the Golgi apparatus, either in drug induced-MDR cells (Molinari *et al*., 1994) or in intrinsic drug resistant cells, such as melanoma cells, seems to exert a transport activity, as supported by the effects of MDR-modifiers. Thus, the hypothesis that Pgp in the Golgi apparatus represents, if not a decisive, a complementary protective mechanism against toxic agents in chemotherapy-refractory malignant melanoma, seems to be supported.

Acknowledgements

This work was partially supported by National Research Council (CNR), Special Project ACRO, contract 96.00665.39. The authors are greatly indebted to Lamberto Camilli and Laura Toccacieli Baldassarri for the valuable technical assistance.

References

Arancia G, Bordi F, Calcabrini A, Cametti C, Diociaiuti M and Molinari A (1994) Influence of anthracyclinic antibiotics on membranes of human erythrocytes: a combined radiowave electrical conductivity and electron microscopy study. Bioelectrochem. Bioenerg 34: 45–51.

Arancia G, Bordi F, Calcabrini A, Diociaiuti M and Molinari A (1995) Ultrastructural and spectroscopic methods in the study of anthracycline-membrane interaction. Pharmacol Res 32: 255–272.

Arancia G, Molinari A, Crateri P, Calcabrini A, Silvestri L and Isacchi G (1988) Adriamycin-plasma membrane interaction in human erythrocytes. Eur J Cell Biol 47: 379–387.

Baldini N, Scotlandi K, Serra M, Shikita T, Zini N, Ognibene A, Santi S, Ferracini R and Maraldi NM (1995) Nuclear immunolocalization of P-glycoprotein in multidrug-resistant cell lines showing similar mechanisms of doxorubicin distribution. Eur J Cell Biol 68: 226–239.

Beck WT, Danks MK, Yalowich JC, Zamora JM and Cirtain MC (1989) Different mechanisms of multiple drug resistance in two human leukemic cell lines. In: Mechanisms of Multiple Drug Resistance in Neoplastic Cells (pp. 211–220), Academic Press, New York.

Boiocchi M and Toffoli G (1992) Mechanism of multidrug resistance in human tumour cell lines and complete reversion of cellular resistance. Eur J Cancer 28A: 1099–1105.

Breuninger LM, Saptarshi P, Gaughan K, Miki T, Chan A, Aaronson SA and Kruh GD (1995) Expression of multidrug resistance-associated protein in NIH/3T3 cells confers multidrug resistance associated with increased drug efflux and altered intracellular drug distribution. Cancer Res 55: 5342–5347.

Broxterman HJ, Schurrhuis GJ, Lantelma J, Baak JPA and Pinedo HM (1990) Towards functional screening for multidrug resistant cells in human malignancies. In: Mihich E (ed) Drug Resistance: Mechanism and Reversal (pp. 309–319), John Libbey, CIC, Rome.

Calcabrini A, Villa AM, Molinari A, Doglia SM and Arancia G (1997) Influence of N-methylformamide on the intracellular transport of doxorubicin. Eur J Cell Biol 72: 61–69.

Chaires JB, Dattagupta N and Crothers DM (1982) Interaction of anthracycline antibiotics and DNA. Biochemistry 21: 3933–3940.

Cianfriglia M, Willingham MC, Tombesi M, Scagliotti V, Frasca G and Chersi A (1994) P-glycoprotein mapping. I. Identification of a linear human-specific epitope in the fourth loop of the P-glycoprotein extracellular domain by MM4.17 murine monoclonal antibody to human multi-drug–resistant cells. Int J Cancer 56: 153–160.

Coan DE, Wechezack AR, Viggers RF and Sauvage LR (1993) Effect of shear stress upon localization of the Golgi apparatus and microtubule organizing center in isolated cultured endothelial cells. J Cell Sci 104: 1145–1153.

Coley HM, Amos WB, Twentyman PR and Workman P (1993) Examination by laser scanning confocal fluorescence imaging microscopy of the subcellular localization of anthracyclines in parent and multidrug resistant cell lines. Br J Cancer 67: 1316–1323.

Cornwell MM, Pastan I and Gottesman MM (1987) Certain calcium channel blockers bind specifically to multidrug resistant human KB carcinoma membrane vesicles and inhibit drug binding to P-glycoprotein. J Biol Chem 262: 2166–2170.

De Lange JHM, Schipper NW, Schurrhuis GJ, Ten Kate TK, Jan Heijningen Th HM, Pinedo HM, Lankelma J and Baak JPA (1992) Quantification of intracellular doxorubicin distribution in multidrug resistant and sensitive cells by laserscan microscopy and digital image processing. Cytometry 13: 572–576.

Diociaiuti M, Molinari A, Calcabrini A and Arancia G (1991a) Electron energy-loss spectroscopy analysis of adriamycin-plasma membrane interaction. J Microsc 164: 95–106.

Diociaiuti M, Molinari A, Calcabrini A, Arancia G, Isacchi G, Bordi F and Cametti C (1991b) Alteration of the passive-electrical properties of adriamycin-treated red cell membrane deduced from dielectric spectroscopy. Bioelectrochem Bioenerg 26: 177–192.

Diociaiuti M, Calcabrini A, Meschini S and Arancia G (1997) Intracellular mapping of 4′-deoxy-4′-iododoxorubicin in sensitive and multidrug resistant cells by electron spectroscopic imaging. Micron 28: 389–395.

Duarte-Karim M, Ruysschaert JM and Hildebrand J (1976) Affinity of adriamycin to phospholipids: a possible explanation for cardiac mitochondrial lesions. Biochim Biophys Acta 71: 658–663.

Duffy PM, Hayes MC, Cooper A and Smart CJ (1996) Confocal microscopy of idarubicin localization in sensitive and multidrug-resistant bladder cancer cell lines. Br J Cancer 74: 906–909.

Fojo A, Akiyama S, Gottesman MM and Pastan I (1985) Reduced drug accumulation in multiply drug-resistant human KB carcinoma cell lines. Cancer Res 45: 3002–3007.

Fragu P, Klijanienko J, Gandia D, Halpern S and Armand JP (1992) Quantitative mapping of 4′-iododeoxyrubicin in metastatic squamous cell carcinoma by secondary ion mass spectroscopy (SIMS) microscopy. Cancer Res 52: 974–977.

Frezard F and Garnier-Suillerot A (1991) DNA-containing liposomes as a model for the study of cell membrane permeation by anthracyclines derivatives. Biochemistry 30: 5038–5043.

Fritzsche H, Triebel H, Chaires JB, Dattagupta W and Crothers DM (1982) Studies on interaction of anthracyclines antibiotics and DNA. Biochemistry 21: 3940–3946.

Gervasoni JE Jr, Fields SZ, Krishna S, Baker MA, Rosado M, Thuraisamy K, Hindenburg AA and Taub RN (1991) Subcellular distribution of daunorubicin in P-glycoprotein-positive and -negative drug-resistant cell lines using laser-assisted confocal microscopy. Cancer Res 51: 4955–4963.

Goormaghtigh E and Ruysschaert JM (1984) Anthracycline glycoside-membrane interactions. Biochim Biophys Acta 779: 271–288.

Guffy MM, North JA and Burns CP (1984) Effects of cellular fatty acids alteration on adriamycin sensitivity in cultured L1210 murine leukemia cells. Cancer Res 44: 1863–1866.

Henry N, Fantine EO, Bolard J and Garnier-Suillerot A (1985) Interaction of adriamycin with negatively charged model membranes: evidence of two types of binding sites. Biochemistry 24: 7085–7092.

Hindenburg AA, Gervasoni JE Jr, Krishna S, Stewart VJ, Rosado M, Lutzky J, Bhala K, Baker MA and Taub RN (1989) Intracellular distribution and pharmacokinetics of daunorubicin in anthracycline-sensitive and -resistant HL60 cells. Cancer Res 49: 4607–4614.

Huxham HG, Pinedo HM, Schuurhuis GJ and Joenje H (1992) The use of parallel EELS spectral imaging and elemental mapping in the rapid assessment of anti-cancer drug localization. J Microsc 166: 367–380.

Keizer HG, Schurrhuis GJ, Broxtermann HJ, Landelma J, Schoonen WGEJ, van Rijn T, Pinedo HJ and Joenje H (1989) Correlation of multidrug resistance with decreased drug accumulation, altered subcellular drug distribution, and increased P-glycoprotein expressed in cultured SW-1573 human lung tumor cells. Cancer Res 49: 2988–2993.

Koh HK (1991) Cutaneous melanoma. New Engl J Med 325: 171–182.

Lewis W and Gonzales B (1986) Anthracycline effects on actin and actin containing thin filaments in cultured neonatal rat myocardial cells. Lab Invest 54: 416–423.

Lothstein L, Wright HM, Sweatman TW and Israel M (1992) N-benzyladriamycin-14-valerate and drug resistance: correlation of anthracycline structural modification with intracellular accumulation and distribution in multidrug resistant cells. Oncol Res 4: 341–347.

Meschini S, Molinari A, Calcabrini A, Citro G and Arancia G (1994) Intracellular localization of the antitumour drug adriamycin in living cultured cells: a confocal microscopy study. J Microsc 176: 204–210.

Mizuno NS, Zakis B and Decker RW (1975) Binding of daunomycin to DNA and the inhibition of RNA and DNA synthesis. Cancer Res 35: 1542–1546.

Molinari A, Calcabrini A, Crateri P and Arancia G (1990) Interaction of anthracyclinic antibiotics with cytoskeletal components of cultured carcinoma cells. Exp Mol Pathol 53: 11–33.

Molinari A, Calcabrini A, Crateri P and Arancia G (1991) Effects of daunomycin on the microtubular network: a cytochemical study on a human melanoma cell line. Eur J Cell Biol 54: 291–298.

Molinari A, Cianfriglia M, Meschini S, Calcabrini A and Arancia G (1994) P-glycoprotein expression in the Golgi apparatus of multidrug-resistant cells. Int J Cancer 59: 789–795.

Molinari A, Calcabrini A, Meschini S, Stringaro A, Del Bufalo D, Cianfriglia M and Arancia G (1998) Detection of P-glycoprotein in the Golgi apparatus of drug-untreated human melanoma cells. Int J Cancer 75: 885–893.

Monparler RL, Karon M, Siegel SE and Avila E (1976) Effects of adriamycin on DNA, RNA and protein synthesis in cell free systems and intact cells. Cancer Res 36: 2891–2895.

Oth D, Begin M, Bischoff P, Leroux JY, Mercier G and Bruneau C (1987) Induction by adriamycin and mitomycin C of modifications in lipid composition, size distribution, membrane fluidity and permeability of cultured RDM4 lymphoma cells. Biochim Biophys Acta 900: 198–208.

Peterson C and Trouet A (1978) Transport and storage of daunorubicin and doxorubicin in cultured fibroblasts. Cancer Res 38: 4645–4649.

Rabkin SW and Sunga P (1987) The effects of doxorubicin (adriamycin) on cytoplasmic microtubule system in cardiac cells. J Mol Cell Cardiol 19: 1073–1083.

Ralph WE, Marshall B and Darkin S (1983) Anticancer drugs which intercalate DNA: how do they act? TIBS 8: 212–214.

Rutherford AV and Willingham MC (1993) Ultrastructural localization of daunomycin in multidrug resistant cells with modulation of the multidrug transporter. J Histochem Cytochem 41: 1573–1577.

Saeki T, Ueda K, Tanigawara Y, Hori R and Komano T (1993) Human P-glycoprotein transports cyclosporin A and FK506. J Biol Chem 268: 6077–6080.

Safa AR, Glover CJ, Sewell JL, Meyers MB, Biedler JL and Felsted RL (1987) Identification of the multidrug resistance-related membrane glycoprotein as an acceptor for calcium channel blocker. J Biol Chem 262: 7884–7888.

Schadendorf D, Makki A, Stahr C, van Dick A, Wanner R, Scheffer GL, Flens MJ, Scheper R and Henz BM (1995) Membrane transport proteins associated with drug resistance expressed in human melanoma. Am J Pathol 147: 1545–1552.

Scheper RJ, Broxterman HJ, Scheffer JL, Kaaijk P, Dalton WS, van Heiningen THM, van Kalken CK, Slovack ML, De Vries EGE, van der Valk P, Meijer CJLM and Pinedo HM (1993) Overexpression of a 110 kD vesicular protein in non-P-glycoprotein mediated multidrug resistance. Cancer Res 53: 1475–1479.

Schurrhuis GJ, Broxteman HJ, Cervantes A, van Heijningen THM, de Lange JHM, Baak JPA, Pinedo HM and Lankelma J (1989) Quantitative determination of factors contributing to doxorubicin resistance in multidrug-resistant cells. J Natl Cancer Inst 81: 1887–1892.

Schurrhuis GJ, Broxteman HJ, de Lange JHM, Pinedo HM, van Heijningen THM, Kuiper CK, Baak JPA and Lankelma J (1991) Early multidrug resistance, defined by changes in intracellular doxorubicin distribution, independent of P-glycoprotein. Br J Cancer 64: 857–861.

Schurrhuis GJ, van Heijningen THM, Cervantes A, Pinedo HM, de Lange JHM, Keizer HG, Broxteman HJ, Baak JPA and Lankelma J (1993) Changes in subcellular doxorubicin distribution and cellular accumulation alone can largely account for doxorubicin resistance in SW-1573 lung cancer and MCF-7 breast cancer multidrug resistant tumor cells. Br J Cancer 68: 898–908.

Sehested M, Skovsgaard T, van Deurs B and Winther-Nielsen H (1987) Increase in nonspecific adsorptive endocytosis in anthracycline- and vinca alkaloid-resistant Ehrlich ascites tumor cell lines. J Natl Cancer Inst 78: 171–179.

Seidel A, Hasmann M, Loser R, Bunge A, Schaefer B, Herzig I, Steidtmann K and Dietel M (1995) Intracellular localization, vesicular accumulation and kinetics of daunorubicin in sensitive and multidrug-resistant gastric carcinoma EPG85-257 cells. Wirchows Archiv 426: 249–256.

Siegfried J, Kennedy AK, Sartorelli AC and Tritton TR (1983) The role of membranes in the mechanism of action of the antineoplastic agent adriamycin. J Biochem Chem 258: 339–343.

Toffoli G, Corona G, Simone F, Gigante M, De Angeli S and Boiocchi M (1996) Cellular pharmacology of idarubicinol in multidrug-resistant LoVo cell lines. Int J Cancer 67: 129–137.

Tritton TR and Yee G (1982) The anticancer agent adriamycin can be actively cytotoxic without entering the cells. Science 217: 248–250.

White JG, Amos WB and Fordham M (1987). An evaluation of confocal vs conventional imaging of biological structures by fluorescence light microscopy. J Cell Biol 105: 41–48.

Willingham MC, Cornwell MM, Cardarelli CO, Gottesman MM and Pastan I (1986) Single cell analysis of daunomycin uptake and efflux in multidrug-resistant and -sensitive KB cells: effect of verapamil and other drugs. Cancer Res 46: 5941–5946.

Willingham MC, Richert ND, Cornwell MM, Tsuruo T, Hamada H, Gottesman MM and Pastan I (1987) Immunocytochemical localization of P170 at the plasma membrane of multidrug-resistant human cells. J Histochem Cytochem 35: 1451–1456.

Wilson T (1990). Confocal microscopy. Academic Press Inc, San Diego.

Zaman GRL, Versantvoort OHM, Smit JJM, Eijdems EWHM, De Haas M, Smith AJ, Broxterman HJ, Mulder NH, De Vries EGE, Baas F and Borst P (1993) Analysis of the expression of MRP, the gene for a new putative transmembrane drug transporter, in human multidrug resistant lung cancer cell lines. Cancer Res 53: 1747–1750.

Address for correspondence: Giuseppe Arancia, Department of Ultrastructures, Istituto Superiore di Sanità, Viale Regina Elena 299, 00161 Rome, Italy.